Kinetics and Mechanism of the Recognition of Endotoxin by Polymyxin B

Celestine J. Thomas,[†] Beechanahalli P. Gangadhar,[†] Namita Surolia,[‡] and Avadhesha Surolia*,[†]

Contribution from the Molecular Biophysics Unit, Indian Institute of Science, Banglore 560 012, India, and Jawaharlal Nehru Centre for Advanced Scientific Research, Jakkur Campus, Jakkur P.O., Banglore 560 012, India

Received May 21, 1998

Abstract: We report here, for the first time, the elementary steps involved in the recognition of the endotoxin (lipopolysaccharide) molecule by polymyxin B (PMB), a cyclic cationic decapeptide. Miniscule amounts of lipopolysaccharide, the invariant structural component of Gram-negative bacterial outer membranes, in circulation in humans elicits "endotoxic shock" syndrome, which is fatal in almost 60% of the instances. PMB, despite its harmful side effects, is the only useful drug for combating endotoxic shock. It neutralizes the endotoxin by binding to it. The kinetics and mechanism of this important biological recognition, investigated by stopped-flow spectrofluorometry, provide considerable insight about the endotoxin neutralizing activity of this antibiotic. This process consists of a pair of kinetically distinguishable but consecutive association and dissociation reactions, with rate constants of 1.98×10^5 M^{-1} s^{-1} (k_1), 0.458 s^{-1} (k_2), 0.458 s^{-1} (k_{-1}), and 0.0571 s^{-1} (k_{-2}) at 20 °C. Analysis of the activation parameters for this recognition suggests that, during the first phase of the reaction, which is bimolecular in nature, PMB associates with endotoxin in a relatively less constrained manner. Subsequently, a considerable reorganization of this initial complex occurs, which entails a significant expenditure of energy. Design of analogues of PMB which are able to overcome the constraints of the rate-limiting step should serve as more effective agents for treating endotoxic shock.

Introduction

Lipopolysaccharides (LPS), major structural components of Gram-negative bacterial outer membranes,[1−5] manifest a multitude of toxic effects in a wide of variety organisms, from insects to humans.[6] The release of LPS into systemic circulation in humans, a sequel of major Gram-negative infections, leads to a plethora of symptoms termed "endotoxic shock", which is characterized by hemodynamic abnormalities, coagulopathy, and multiple system organ failure.[7] Endotoxic shock accounts for up to 60% fatalities in humans.[8] Pleiotropic effects of LPS on the susceptible organisms/tissues include B-cell mitogenesis, activation of complement, release of cytokines, mimicry of acute-graft versus host disease, pyrogenicity in mammals, and triggering of the defense and clotting cascade in the horseshoe crab.[9,10]

Through total organic synthesis, it has been established unambiguously that the amphiphilic lipid A moiety, an acylated phosphodisaccharide unit, common to all the Gram-negative bacterial LPS, constitutes the toxic component of the endotoxin.[9,11] Consequently, sequesteration of LPS through agents that interact with it strongly and specifically constitutes an important interventional strategy for combating endotoxic shock.[12−21] Among several substances that are known to bind to LPS, polymyxin B (PMB), a cyclic cationic decapeptide antibiotic, and its analogues obtained from *Bacillus polymyxa* have been used with some success in severe cases of sepsis.[22−24]

* Corresponding author. E-mail: surolia@mbu.iisc.ernet.in. Telephone: 080-309-2389.

[†] Indian Institute of Science.

[‡] Jawaharlal Nehru Centre for Advanced Scientific Research. E-mail: surolia@jncasr.ac.in. Telephone: 080-846-2750-55.

(1) Lieve L. *Ann. N. Y. Acad. Sci*. **1974**, *235*, 109−129.

(2) Sanderson, K. E.; MacAlister, T. J.; Costerton. J. W. *Can. J. Microbiol.* **1974**, *14*, 239−334.

(3) Galanos, C.; Luderrzitz, O.; Rietschel. E. T.; Westphal O. *Int. Rev. Biochem*. **1977**, *14*, 239−334.

(4) Westphal, O. *Trans. Coll. Int. Aller.* **1975**, *49*, 1−43.

(5) Raetz, C. R. H. *Annu. Rev. Biochem.* **1990**, *59*, 129−170.

(6) Morrison, D. C.; Rudbach, J. A, *Contemp. Top. Mol. Immunol.* **1981**, *8*, 187−218

(7) Fink, P. F. Sepsis Syndrome. In *Handbook of Critical Care*, 3rd ed.; Berk, J. L., Sampliner, J. E., Eds.; Little, Brown & Co.: Boston, 1990; p 619.

(8) Zeigler, E. T.; et al. *N. Engl. J. Med.* **1991**, *324*, 429−436.

(9) Reitschel, E. T.; Brade, H. *Sci. Am.* **1992,** *7*, 26−33.

(10) Iwanaga, S. *Curr. Opin. Immunol*. **1993**, *1*, 74−84.

(11) Neter, E. O.; Westphal, O.; Luderitz, E. A.; Gorzynski,; Cohenberger, E. *J. Immunol*. **1956**, *11*, 377−385.

(12) Cross, A. S.; Opal, S. *J. Endotoxin. Res.* **1994**, *1*, 57−69

(13) Dentener, M. A.; et al. *J. Immunol*. **1993**, *151*, 4258−4265.

(14) Elsbach, P.; Weiss, *J. Immunobiol.* **1993,** *187*, 417−429.

(15) Fisher, C. J., Jr.; Marra, M. A.; Palardy, J. E.; Marchbanks, C. R. *Crit. Care Med*. **1994**, *22*, 553−558.

(16) Nelson, D.; Kuppermann, N.; Fleisher, G. R.; et al. *Crit. Care Med.* **1995**, *23*, 92−98.

(17) Christ, W. J.; Asano, O.; Robidoux, A. L. C.; et al. *Science* **1995**, *268*, 80−83.

(18) Kirikae, T.; Schade, F. U.; Kirikae, F.; Qureshi, N.; Takayama, K.; Reitschel, E. T. *FEMS Immunol. Med. Microbiol.* **1994**, *9*, 237−224.

(19) Loppnow, H.; Libby, P.; Freudenberg, M.; Kruss, J. H.; Weckesser, J.; Mayor, H. *Infect. Immun*. **1990**, *58*, 3743−3750.

(20) Novogrodsky, A.; Vanichkin, A.; Patya, M.; Gazit, A. Osherov, N.; Levitzki, A. *Science* **1994**, *264*, 1319−1322.

(21) Quezado, Z. M. N.; Banks, S. M.; Natanson, C. *Trends. Biotechnol*. **1995**, *13*, 56−63.

(22) Morrison, D. C.; Jacobs, D. M. *Immunochemistry* **1976**, *13*, 813−818.

(23) Schindler, M.; Osborn, M. J. *Biochemistry* **1979**, *18*, 4425−4430.

(24) Schindler, M.; Teuber, M. *Antimicrob. Agents Chemother*. **1975**, *8*, 95−104.

10.1021/ja981777j CCC: $15.00
Published on Web 12/09/1998

Despite the strong and stoichiometric binding of PMB to LPS,[25,26] its use in treating sepsis is severely compromised due to its severe toxicity,[27] because of the harmful side effects associated with its slow degradation in vivo, attributed to the presence of a large fraction of uncommon D-amino acids and its unusual covalent structure.[28]

There have been numerous attempts to explain the relationship between the structure of PMB and its function.[29−32] These studies have led to the suggestion that its amphiphilic nature is responsible for its specific interaction with LPS. Despite these efforts, the exact mode of PMB−LPS interaction has not yet been clearly elucidated. Binding of PMB to LPS has been studied by displacement of fluorescent probes and other techniques.[26,33,34] However, no attempt has been made to elucidate the kinetics and the mechanisms involved therein. As knowledge of the elementary steps and the activation parameters involved in the macromolecule−ligand interactions provides invaluable insights on this biological recognition processes and aids in the design of molecules with improved activities, we report the stopped-flow analyses of this reaction. These studies show that the binding of PMB to LPS consists of a pair of kinetically distinguishable association and dissociation reactions. These reactions are mostly entropically controlled, with hydrophobic forces playing a vital role. These studies thus not only rationalize the events involved in the association of PMB with LPS vis à vis its structural features but also should serve the goal of designing more potent LPS neutralizing agents.

Results

When dansyl-PMB was titrated with increasing concentrations of LPS, its fluorescence intensity at 495 nm was raised progressively, until saturation was achieved (Figure 1a). Fluorescence resonance energy transfer (FRET) between the fluorescein and the rhodamine fluorophores occurs when fluorescein-labeled LPS is mixed with rhodamine-PMB (Figure 1c). These changes in fluorescence intensities were reversed completely when the unlabeled PMB was added to the complex, showing that the binding is due to a specific interaction between LPS and PMB. From the LPS concentration-dependent changes in the fluorescence of dansyl-PMB, the value of the association constant (K_a) was calculated according to the method of Chipman et al.[35] by plotting $\log[(F_o - F_c)/(F_\alpha - F_o)]$ versus $\log [LPS]_f$ using eq 1, where F_o and F_c are fluorescence

$$\log\{(F_o - F_c)/(F_\alpha - F_o)\} = \log\{[LPS]_t - (\Delta F/\Delta F_m)[P]_t\} + \log K_a \quad (1)$$

intensities of free dansyl-PMB and at a particular concentration of LPS, respectively. ΔF_m is the maximum change in fluorescence when all the ligand molecules are complexed with LPS. $[LPS]_t$ and $[P]_t$ represent the total concentrations of LPS and dansyl-PMB, respectively. The values of K_a and stoichiometry (n) for the dansyl-PMB−LPS interaction thus obtained were 2.1×10^6 M^{-1} and 1, respectively, when LPS molecular weight was taken to be 20 000. These values are in agreement with earlier studies of PMB−LPS interaction, excepting one report, with respect to n, which is perhaps related to the differences in the experimental conditions employed.[23,25,26] Similar values of K_a (2.3×10^6 M^{-1}) and n (1) were obtained with FRET. Hence, most experiments were conducted by monitoring the changes in the fluorescence of dansyl-PMB on binding to LPS.

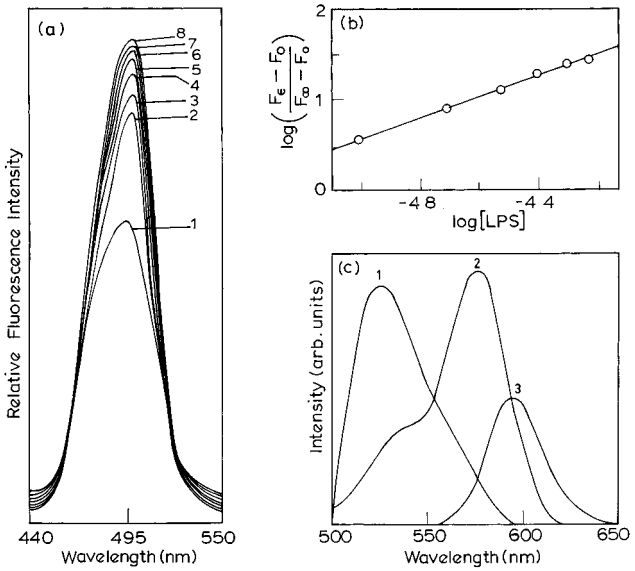

Figure 1. Interaction of fluorescently labled PMB with LPS at 20 °C. (a) Fluorescence spectra of 1-mL solution of 8 μM dansyl-PMB titrated with 20, 40, 60, 80, 100, 120, 140, and 150 μL of LPS (100 μM) are shown in curves 1−8, respectively. (b) Chipman[35] plot for the fluorescence titration of dansyl-PMB with LPS. Linear regression of the plot gives $K_a = 2.06 \times 10^6$ M^{-1}. (c) Observation of FRET when rhodamine-labled PMB was complexed with FITC-LPS. Spectrum 1 shows the overlap between the fluorescence spectrum of FITC and the excitation spectrum (2) of rhodamine when FITC-LPS complexed with rhodamine-PMB was excited at 495 nm.

Kinetic Studies. A typical stopped-flow trace for the association of PMB with LPS is shown in Figure 2. Fit of these transients to a biexponential reaction alone yields data of good quality (Figure 2a). The values of k_1 at varying concentrations of dansyl-PMB (10−75 μM; LPS 1 μM) were in the range of 1.03×10^5−5.5×10^5 M^{-1} s^{-1},whereas the values of k_2 were invariant (0.336 s^{-1}) at all concentrations of excess component. For the FRET-based experiments (fluorescein-labled LPS 2 μM; dansyl-PMB 15 μM), values of k_1 and k_2 were 1.6×10^5 M^{-1} s^{-1} and 0.31 s^{-1}, respectively. Similar values of k_1 and k_2 were obtained when LPS (5−100 μM; dansyl-PMB 3 μM) was used as the excess component. A first-order plot for a typical dissociation reaction for the displacement of dansyl-PMB bound to LPS with the excess concentration of unlabeled PMB also exhibits two well-resolved phases. (Figure 3, inset) The dissociation rates k_{-1} and k_{-2} thus obtained were 0.458 and 0.057 s^{-1}, respectively, at 20 °C. These values remained

(25) Rustici, A.; Velucchi, M.; Faggioni, R.; Sironi, M.; Ghezzi, P.; Quataert, S.; Green, B.; Porro, M. *Science* **1993**, *259*, 361−365.
(26) Srimal, S.; Surolia, N.; Balasubramaian, S.; Surolia, A. *Biochem. J.* **1996**, *315*, 679−686.
(27) Rifkind, D. *J. Bacteriol.* **1967**, *93*, 1463−1464.
(28) Storm, D. R.; Rosenthal, K. S.; Swanson, P. E. *Annu. Rev. Biochem.* **1977**, *46*, 723−763.
(29) Schroder, G.; Brandenburg, K.; Seydel, U. *Biochemistry* **1992**, *31*, 631−638.
(30) Hartmann, W.; Galla, H. J.; Sackmann, E. *Biochim. Biophys. Acta* **1978**, *510*, 124−139.
(31) Chapman, T. M.; Golden, M. R. *Biochem. Biophys. Res. Commun.* **1972**, *46*, 2040−2047.
(32) Galardy, R. E.; Craig, L. C.; Printz, M. P. *Biochemistry* **1974**, *12*, 1674−677.
(33) Richard, A. M.; Nancy, C. B.; Robert, E. W. H. *Antimicrob. Agents Chemother*. **1986**, *29*, 496−500.
(34) David, S. A.; Balasubramanian, K. A.; Mathan, V. I.; Balaram, P. *Biochim. Biophys. Acta* **1992**, *1165*, 147−152.
(35) Chipman, D. M.; Grisaro, V.; Sharon, N. *J. Biol. Chem*. **1967**, *242*, 2819−2822.

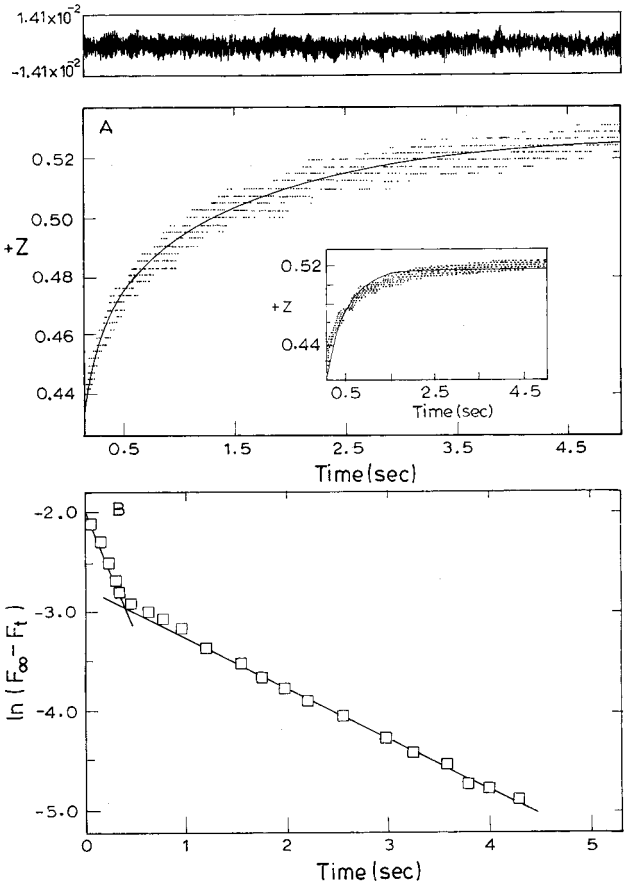

Figure 2. Stopped-flow trace for the association reaction of dansyl-PMB with LPS at 30 °C. (a) The association reaction was intiated by mixing equal volumes of dansyl-PMB (10 μm) and LPS (1 μM) in the stopped-flow cell. The samples were excited at 340 nm and emission was recorded above 450 nm. The spectrum represents the average of 10 measurements. Continuous line is the nonlinear least-squares fit of the data to a biexponential equation. Residuals for the biexponential fit are shown in the top panel. k_1 and k_2 were found to be 3.05×10^5 M^{-1} s^{-1} and 0.668 s^{-1}, respectively. Inset shows the fit of the trace to a monoexponential equation which has an unacceptable distribution of residuals. (b) A plot of $F_\infty - F_t$ versus time according to eq 2, which clearly depicts the biphasic binding pattern of the interaction of LPS with dansyl-PMB.

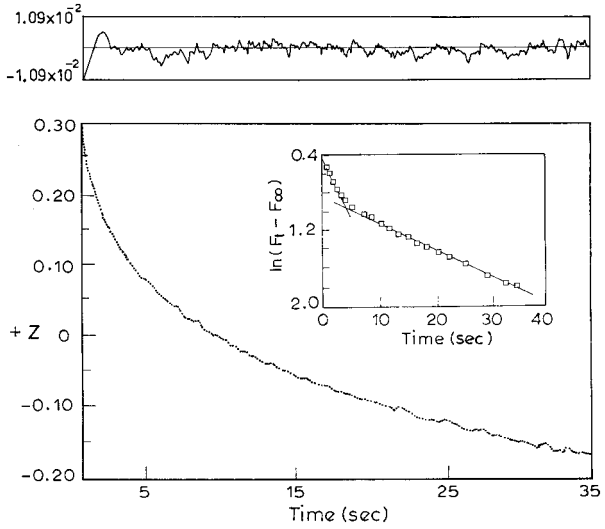

Figure 3. Stopped-flow fluorescence trace for the dissociation of dansyl-PMB−LPS complex by a large excess of PMB at 25 °C. For the displacement reaction, equal volumes of dansyl-PMB−LPS complex (5 μM) and unlabeled PMB (1 mM) were mixed in the stopped-flow cell, and the change in the fluorescence was monitored as stated above. Continuous line is the biexponential fit of the data. k_{-1} and k_{-2} were found to be 0.486 and 0.588 s^{-1}, respectively. Residuals are shown in the top panel. Inset shows the time dependence of the change in fluorescence, which also indicates the biphasic pattern of the dissociation process.

invariant when the concentration of PMB was altered (1−10 mM) or the amount of dansyl-PMB−LPS complex was varied (10−75 μM).

The biphasic nature for the binding of dansyl-PMB with LPS is also apparent when the data are analyzed according to eq 2 by plotting the change in fluorescence ($F_\infty - F_t$) with

$$F_\infty - F_t = B e^{\lambda_1 t} + (F_\infty - F_t - B) e^{\lambda_2 t} \qquad (2)$$

respect to time, where F_∞ and F_t are fluorescence at infinite time and at time t, respectively. The reciprocal of relaxation times, λ_1 and λ_2, corresponds with the fast and slow phases of change in fluorescence, respectively, which are shown in Figure 2b. The value of λ_1 increases linearly, while that of λ_2 remains constant with increasing concentration of the dansyl-PMB, the excess component (Figure 4a). The biphasic nature of reaction remains both quantitatively and qualitatively unchanged when LPS is used as the excess component. Hence, the heterogeneity in either of the reactants can be ruled out as being responsible for the observed biphasicity. Occurrence of the biphasisity for the binding of dansyl-PMB (P), the component in excess, with LPS or lipid A (L) could be analyzed in terms of pathways 1−5.

$$\mathrm{P} + \mathrm{L} \underset{k_{-1}}{\overset{k_1}{\rightleftharpoons}} \mathrm{PL} \underset{k_{-2}}{\overset{k_2}{\rightleftharpoons}} \mathrm{PL}^* \qquad \text{Pathway 1}$$

$$\mathrm{PL}^* \underset{k_{-1}}{\overset{k_1}{\rightleftharpoons}} \mathrm{P} + \mathrm{L} \underset{k_{-2}}{\overset{k_2}{\rightleftharpoons}} \mathrm{PL} \qquad \text{Pathway 2}$$

In pathway 1, the initial complex isomerizes to the final complex. In pathway 2, two different complexes (PL and PL*) form at relative rates equal to the ratio k_{-1}/k_2, which during the slow phase equilibrate so that the concentrations of PL* and PL approach the equilibrium ratio $k_1k_{-2}/k_{-1}k_2$.

$$\mathrm{P} \underset{k_{-1}}{\overset{k_1}{\rightleftharpoons}} \mathrm{P}^* + \mathrm{L} \underset{k_{-2}}{\overset{k_2}{\rightleftharpoons}} \mathrm{PL}^* \qquad \text{Pathway 3}$$

In pathway 3, the excess component, the peptide, undergoes a slow transformation between two states, of which only P* is able to associate with L. For this pathway, λ would decrease as P increases, and only one relaxation time would be observed. Hence, this pathway can be ruled out.

$$\mathrm{P} + \mathrm{L} \underset{k_2}{\overset{k_1}{\rightleftharpoons}} \mathrm{PL}^*_1 \quad \text{and} \quad \mathrm{P} + \mathrm{L} \underset{k_{-1}}{\overset{k_{-2}}{\rightleftharpoons}} \mathrm{PL}^*_2 \qquad \text{Pathway 4}$$

In pathway 4, two mutually exclusive complexes are formed so that one bound form precludes the other from occurring. Each reaction involves bimolecular binding of the peptide with the lipid and requires dissociation from a given complex before it can engage itself in a different binding mode. The two on rates for this process are expected to be concentration dependent and could have very similar rates. The differences in the two off rates would determine the affinities of the two complexes. This scheme, however, can be ruled out by the fact that it

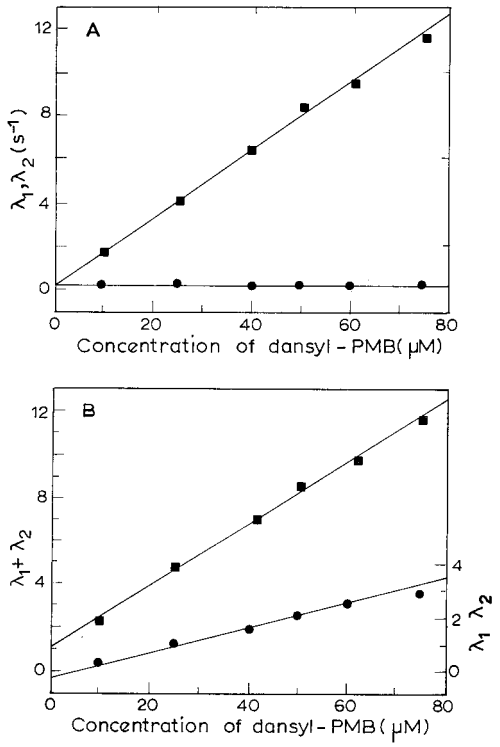

Figure 4. Concentration dependence of λ_1 and λ_2. (a) λ_1 (■) shows marked concentration dependence, while λ_2 (●) shows no concentration dependence.Concentration of dansyl-PMB ranged from 10 to 75 μM. Values are derived from an average of 10 stopped-flow traces. (b) Linear least-squares fit of a plot of $\lambda_1 + \lambda_2$ (■) versus [dansyl-PMB] to obtain m_s the for slope and b_s for the intercept. Linear least-squares fit of the plot of $\lambda_1\lambda_2$ (●) versus [dansyl-PMB] to obtain m_p for the slope and b_p for the intercept.

invokes two on rates that are concentration dependent as well as by the fact that the plots of λ_1 or λ_2 as a function of the excess component would be linear for the fast component and would plateau off from an initial linear phase for the second one.

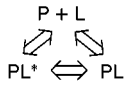

Pathway 5

Pathway 5 constitutes a combination of pathways 1 and 2 which invokes a shift in the equibrium between two forms of the peptide. However, it is unlikely to occur, as only two distinct kinetic steps are observed instead of the three required by the scheme. Even if the kinetic constants for these reactions were such as to give only two relaxation times, pathway 5 is ruled out by our failure to observe two on rates that are dependent on the concentration of the excess component. Moreover, the symmetric reversal of the excess component should have altered the faster relaxation time.

In summary, the observation of two on rates, of which only one is concentration dependent, and two off rates, together with the consideration outlined above, leaves us with the mechanisms outlined in pathways 1 and 2 as the most likely ones consistent with these data (Figures 2−4). The analyses outlined below help to resolve which one of them is most likely to occur. Since [P] ≥ 10[L], pathways 1 and 2 are analyzed as consecutive pseudo-first-order reactions. Though λ_1 and λ_2 are each related to the four rate constants in a complex manner, their sum is linearly dependent on P and the given rate constants for pathways 1 and 2, as shown by eqs 3 and 4, respectively.[36] The

$$\lambda_1 + \lambda_2 = k_{-1} + k_{-2} + k_2 + k_1[\mathrm{P}] \tag{3}$$

$$\lambda_1 + \lambda_2 = k_1 + k_{-2} + (k_{-1} + k_2)[\mathrm{P}] \tag{4}$$

slope and intercept of a plot of $\lambda_1 + \lambda_2$ vs [P] yields k_1 and $(k_{-1} + k_{-2} + k_{+2})$ for pathway 1 and $(k_{-1} + k_{-2})$ and $(k_1 + k_{-2})$ for pathway 2, respectively (Figure 4b). The product $\lambda_1\lambda_2$ also is a linear function of [P] and bears a simple relationship to the individual rate constants for pathways 1 and 2, as shown by eqs 5 and 6, respectively[36] (Figure 4b). A linear least-squares

$$\lambda_1\lambda_2 = k_1k_{-2} + (k_1k_2 + k_{-1}k_{-2})[\mathrm{P}] \tag{5}$$

$$\lambda_1\lambda_2 = k_{-1}k_{-2} + k_1(k_2 + k_{-2})[\mathrm{P}] \tag{6}$$

fit of a plot of $\lambda_1 + \lambda_2$ vs [P] yields values of $m_s = (2.0 \pm 0.08) \times 10^5\ \mathrm{M^{-1}\ s^{-1}}$ for the slope and $b_s = 1.3 \pm 0.10)\ \mathrm{s^{-1}}$ for the intercept. A linear least-squares fit for a plot of $\lambda_1\lambda_2$ vs [P] yields values of $m_p = 4.2 \pm 0.15) \times 10^4\ \mathrm{s^{-2}\ M^{-1}}$ and $b_p = 0.01 \pm 0.2\ \mathrm{s^{-2}}$ for the slope and intercept, respectively (Figure 4a). Two relaxation times associated with the displacement reaction, $\lambda_{1\ \mathrm{off}}$ and $\lambda_{2\ \mathrm{off}}$, are related by eqs 7 and 8, respectively, to the intercept (b_s) of the plot of $\lambda_1 + \lambda_2$ vs [P] and the intercept (b_p) of $\lambda_1\lambda_2$ vs [P] (Figure 4b).

$$\lambda_{1\ \mathrm{off}} = b_s + (b_s^{\,2} - 4b_p)^{0.5}/2 \tag{7}$$

$$\lambda_{2\ \mathrm{off}} = b_s - (b_s^{\,2} - 4b_p)^{0.5}/2 \tag{8}$$

The individual rate constants for pathway 1 are calculated as follows:

$$k_1 = m_s;\quad k_{-1} = b_s - m_p/m_s$$
$$k_{-2} = b_p/k_{-1};\quad \text{and}\quad k_2 = m_p/m_s - k_{-2}$$

where m_s and b_s and m_p and b_p are the slopes and intercepts of plots of $\lambda_1 + \lambda_2$ vs [P] and $\lambda_1\lambda_2$ vs [P], respectively. The individual rate constants for pathway 2 are calculated as follows:

$$k_1 = b_s - k_{-2};\quad k_{-1} = m_s - k_{+2}$$
$$k_2 = (m_p - m_sk_{-2})/(k_1 - k_{-2})$$
$$\text{and}\quad k_{-2} = (b_s - (b_s^{\,2} - 4b_p)^{0.5})/2$$

As shown in eqs 9 and 10, the ratio of slope to intercept of a plot of $\lambda_1\lambda_2$ vs [P] yields the value of the overall equilibrium constant, K_a, for pathways 1 and 2, respectively. The values

$$K_a = \frac{[\mathrm{PL}] + [\mathrm{PL}^*]}{[\mathrm{P}][\mathrm{L}]} = \frac{k_1}{k_{-1}}\left(\frac{k_2}{k_{-2}} + 1\right) \tag{9}$$

$$K_a = \frac{[\mathrm{PL}] + [\mathrm{PL}^*]}{[\mathrm{P}][\mathrm{L}]} = \frac{k_2}{k_{-2}} + \frac{k_{-1}}{k_1} \tag{10}$$

of K_a obtained from the kinetic data ($(1.7 \pm 0.2) \times 10^6\ \mathrm{M^{-1}}$) are in the range of those obtained from the steady-state fluorescence ($(1.9 \pm 0.2) \times 10^6\ \mathrm{M^{-1}}$)$^-$ and titration calorimetry experiments ($K_a = 2.1 \times 10^6\ \mathrm{M^{-1}}$, C. J. Thomas and A. Surolia, data not shown). Values of both the association and dissociation rate constants thus obtained are shown in Table 1. Only k_1 was influenced by an increase in the ionic strength (Table 2).

(36) Willams, T. J.; Shafer, J. A.; Goldstein, I. J.; Adamson, T. *J. Biol. Chem.* **1978**, *253*, 8538−8544.

Table 1. Rate Constants for LPS−dansyl-PMB Interaction Derived for Pathway 1 and Pathway 2 at 20 °C

pathway I, P + L ⇔ PL ⇔ PL*	pathway II, PL* ⇔ P + L ⇔ PL
$k_1 = 1.4 \times 10^5\ M^{-1}\ s^{-1}$	$k_1 = 0.829\ s^{-1}$
$k_2 = 0.56\ s^{-1}$	$k_2 = 8.9 \times 10^4\ M^{-1}\ s^{-1}$
$k_{-1} = 0.31\ s^{-1}$	$k_{-1} = 5.1 \times 10^4\ M^{-1}\ s^{-1}$
$k_{-2} = 0.053\ s^{-1}$	$k_{-2} = 0.072\ s^{-1}$
$K_{a(kin\ 1)}{}^a = 1.712 \times 10^6\ M^{-1}$	$K_{a(kin\ 2)}{}^a = 8.15 \times 10^5\ M^{-1}$
$K_{a(Eq)}{}^b = 2.06 \times 10^6 M^{-1}$	
$K_{b(ITC)} = 2.10 \times 10^6\ M^{-1}$	

[a] $K_{a(kin\ 1)}$ and $K_{a(kin\ 2)}$ are the kinetically determined values of association constants calculated using eqs 11 and 12, respectively. [b] $K_{b(equlibrium)}$ and $K_{b(ITC)}$ are the values obtained by equilibrium fluorescence titrations and ITC experements, respectively, at 20 °C.

Table 2. Influence of Ionic Strength on the Rate Constants of the Association Reaction of dansyl-PMB with LPS at 20 °C[a]

reaction medium	ionic strength of salt added	$k_1 \times 10^{-5}$ ($M^{-1}\ s^{-1}$)	k_2 (s^{-1})
water		6.3	0.400
buffer	0.001	5.2	0.380
buffer + 0.1 M NaCl	0.1	2.0	0.343
buffer + 0.5 M NaCl	0.5	1.9	0.340
buffer + 1.0 M NaCl	1.0	1.9	0.340

[a] Buffer used for this study was 0.1 mM phosphate buffer. All solutions contained 5 μM triethylamine. Rate constants are derived form the Marquardt fit of the stopped-flow traces, utilizing the software provided by the manufacturer, operating on an Acorn A5000, RICS OS, Workstation.

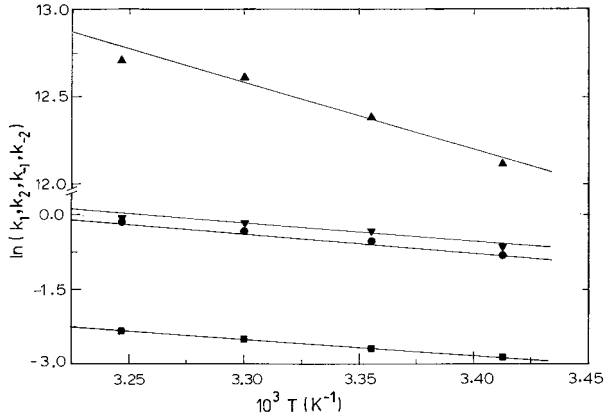

Figure 5. Arrhenius plots of the association and dissociation reactions of the interaction between dansyl-PMB and LPS. In values of the various rate constants i.e., k_1 (▲), k_2 (▼) k_{-1} (●), and k_{-2} (■) are plotted against $1/T \times 10^{-3}$. All rate constants are the mean value of five independent runs. Slopes yield the activation energies for the individual kinetic steps.

The Arrhenius plots for the temperature dependence of various rate constants are shown in Figure 5. The activation parameters obtained according to eqs 11−13 are listed in Table

$$\Delta H = E_a - RT \tag{11}$$

$$\ln(k/T) = -\Delta H/RT + \Delta S/R + \ln(k'/h) \tag{12}$$

$$\Delta G = \Delta H - T\Delta S \tag{13}$$

3, where k is the appropriate rate constant, k' is Boltzman's constant, and h is Planck's constant.

Discussion

These studies are motivated by the assumption that detailed thermodynamic and kinetic analyses of the interaction of PMB with LPS would provide a rationale for its microbicidal and endotoxin neutralization activities. It is, therefore, in order to relate the activity of PMB with its covalent structure, which is shown below, where X corresponds to an acyl (6-methyl-heptanoyl/octanoyl) group and DAB to α,τ-diaminobutyric acid.

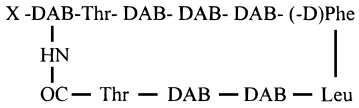

The antimicrobial activity of PMB is a consequence of its interactions with the Gram-negative outer membranes, which are almost entirely comprised of LPS. Subsequent disruption in the packing interactions between the endotoxin molecules culminates in the lysis of the bacterial cell.[24,29,37,38]

It is pertinent here to discuss the phase behavior of LPS/lipid A used in these studies. A wealth of data in the literature indicate that, in the absence of divalent cations such as Ca^{2+} and Mg^{2+}, LPS predominantly exists in a lamellar phase.[39−41] Thus, LPS/lipid A neutralized with triethylamine in aqueous solution used in these studies is predominantly lamellar, as is also proven by the restrictions in the mobilities of fluorescent probes diphenylhexatriene and *N*-phenylnaphthylamine (data not shown).

Our earlier thermodynamic analyses have shown that PMB−LPS interactions, to a large extent, are stabilized by hydrophobic forces, while the positive charges of amino groups of its DAB side chains essentially help to orient appropriately the antibiotic on the surface of LPS during the initial stages of interactions.[26] An enhancement in the fluorescence of the dansyl group of dansyl-PMB shows that it experiences a relatively nonpolar environment. These data are thus consistent with earlier studies

Table 3. Rate Constants and Activation Parameters for the Interaction of dansyl-PMB with LPS[a]

T (°C)	$k_1 \times 10^{-5}$ ($M^{-1}\ s^{-1}$)	k_2 (s^{-1})	k_{-1} (s^{-1})	k_{-2} (s^{-1})	$K_a \times 10^{-6}$ (M^{-1})
20	1.98	0.341	0.458	0.0571	2.5
25	2.51	0.486	0.588	0.0683	2.9
30	3.05	0.668	0.728	0.0834	3.3
35	5.04	0.870	0.979	0.0979	4.6

Association Phase I	Dissociation Phase II
$E_a = 33.71\ kJ\ M^{-1}$	$E_a = 34.47\ kJ\ M^{-1}$
$\Delta H^{\ddagger} = 31.24\ kJ\ M^{-1}$	$\Delta H^{\ddagger} = 32.0\ kJ\ M^{-1}$
$\Delta S^{\ddagger} = -36.69\ J\ K^{-1}\ M^{-1}$	$\Delta S^{\ddagger} = -141.9\ J\ K^{-1}\ M^{-1}$
$\Delta G^{\ddagger} = 42.17\ kJ\ M^{-1}$	$\Delta G^{\ddagger} = 72.2\ kJ\ M^{-1}$
Association Phase II	Dissociation Phase I
$E_a = 54.93\ kJ\ M^{-1}$	$E_a = 27.27\ kJ\ M^{-1}$
$\Delta H^{\ddagger} = 52.46\ kJ\ M^{-1}$	$\Delta H^{\ddagger} = 24.8 kJ\ M^{-1}$
$\Delta S^{\ddagger} = -74.80\ J\ K^{-1}\ M^{-1}$	$\Delta S^{\ddagger} = -183.9\ J\ K^{-1} M^{-1}$
$\Delta G^{\ddagger} = 74.15\ kJ\ M^{-1}$	$\Delta G^{\ddagger} = 79.6\ kJ\ M^{-1}$

$\Delta H° = 26.9\ kJ\ M^{-1}$
$\Delta S° = 213.4\ J\ K^{-1} M^{-1}$
$\Delta G° = -34.88\ kJ\ M^{-1}$

[a] Rate constants are derived form the Marquardt fit of the stopped-flow traces, utilizing the software provided by the manufacturer, operating on an Acorn A5000, RICS OS, Workstation. ITC expriments of dansyl-PMB binding to LPS show a binding constant $K_b = 2.1 \times 10^6\ M^{-1}$, $\Delta H_b = 27.5$ kJ/mol, and stoichiometry of 1.15 at 20 °C.

(37) Teuber, M.; Bader, J. *Arch. Microbiol*. **1976**, *109*, 51−58.
(38) Hai-Ying Wang.; Tummler, B.; Boggs, J. M. *Biochim. Biophys. Acta* **1989**, *985*, 182−198.
(39) Labischinski, H.; Barnickel, G.; Bradaczek, H.; Naumann, D.; Reitschel, E. T.; Giesbrecht, P. *J. Bacteriol*. **1985**, *162*, 9−20.
(40) Seydel, U.; Brandenburg, K.; Koch, M. H. J.; Reitschel, E. T. *Eur. J. Biochem.* **1989**, *186*, 325−332.
(41) Brandenburg, K.; Seydel, U. *Biochim. Biophys. Acta* **1984**, *775*, 225−238.

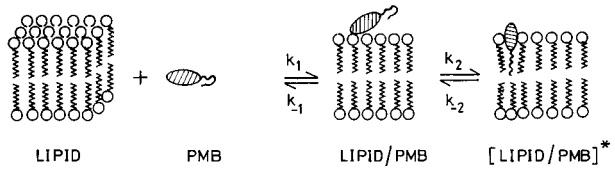

Figure 6. Proposed model for the binding of PMB to LPS. Initial binding of the polymyxim B to the LPS lamellar phase leads to the formation of the intermediate PMB−LPS complex. This complex subsequently isomerizes to yield the final complex, PMB−LPS*, which involves the insertion of the acyl chain of PMB into the LPS lamellar phase.

highlighting the dominance of hydrophobic forces in the stabilization of the complex of PMB with LPS or lipid A.[25,26] These data, taken together with the structural information on PMB, led to the hypothesis that its amphiphilicity, viz., the asymmetric distribution of the nonpolar and the positively charged polar groups in it, is both necessary and sufficient for its binding with the endotoxin molecule.[26,32,42−46] That this is, indeed, the case is proven further by the binding of LPS to a synthetic peptide, where the nonpolar and the polar amino acid side chains are vectorially segregated and which has inconceivable structural similarity with PMB.[47]

The stopped-flow kinetic profiles show two distinct phases for both the association and the dissociation reactions. This indicates that both the association and dissociation reactions proceed through the formation of a kinetically distinguishable intermediate which is both structurally and spectroscopically different from the reactants or the final complex. An examination of the kinetic parameters listed in Table 1 reveals that PMB most likely recognizes endotoxin as depicted in pathway 1.

Figure 6 illustrates a model that accounts for the various kinetic steps involved in the binding of PMB to the endotoxin. According to this scheme, the first step consists of a bimolecular binding step, followed by a monomolecular change. The bimolecular binding step perhaps involves some electrostatic component owing to the presence of negative charges on the LPS molecules and positive charges on the PMB. This is consistent with the diminution in the values of k_1 upon increases in ionic strength. This bimolecular binding step is succeeded by a unimolecular reaction. The latter process is often attributed to a conformational change in the macromolecule, which in most other cases is represented by a protein molecule; however, any unimolecular rearrangement of the complex is possible. According to the scheme outlined in Figure 6, we interpret the unimolecular step to be the insertion of the apolar portion of PMB, including its N-terminal methyloctanoyl/heptanoyl moiety, within the hydrophobic millieu of the endotoxin lamellar phase. Insertion of the hydrophobic component of PMB into the apolar lamellar phase, being the monomolecular step for this reaction, is supported by a host of other studies. PMB, for example, is shown to permeabilize the bacterial cells by disrupting the Gram-negative outer membranes as well as by inducing of polymorphic phase transitions in the LPS assembly.[24,38,47] It also elicits electrically measurable permeability changes in planar bilayers reconstituted with LPS.[29] As the salt has no influence on the rate constant k_2, the monomolecular step does not appear to involve any electrostatic interactions. The proposed mechanism is supported further by studies of the interaction of LPS with polymyxin B nonapeptide, which lacks two N-teminal amino groups and an acyl chain and that perhaps does not display the asymmetric distribution of the apolar and the polar positive charges at disparate regions[47] like PMB. Consequently, it binds to LPS in a single step ($k_1 = 0.5 \times 10^5$ M^{-1} s^{-1}, data not shown).

Agreement between the ΔH values obtained from the ITC experiments and those from kinetic data rules out the occurrence of any additional kinetic step during the reaction that we are not observing but which contributes significantly to the enthalpy of the reaction. The activation parameters thus provide both qualitative and quantitative support to the mechanism proposed for the recognition of LPS by PMB (Table 3).

Conclusion

These results constitute a first step toward understanding the kinetics and mechanism of the binding of PMB with LPS. These studies show that PMB−LPS recognition occurs in two discrete but consecutive steps. In the first phase, the amphipathic PMB molecule approaches the LPS lamellar phase in a process that is relatively sterically unrestrained; viz., it is able to bind to the endotoxin molecule in several orientations. Subsequently, a considerable conformational reorganization of the initial complex occurs. In light of these studies, we believe that design of PMB analogues capable of overcoming the constraints of the rate-limiting step would permit more effective sequesteration of the endotoxin and aid in combating the endotoxic shock

Experimental Section

Materials. All reagents were of analytical grade or ultrapure grade. LPS from *Escherichia coli* strain 55:B5 obtained from Sigma Chemical Co. was repurified according to the phenol−chloroform/petroleum ether extraction method of Galanos et al.[48] The extracted LPS was subjected to a purification protocol as described by Srimal et al.[26] LPS thus prepared had less than 0.009% magnesium, 0.01% of calcium by weight, and contained less than 0.5% protein and 1% nucleic acids.

Fluorescein-labeled LPS was purchased from Sigma Chemical Co. and was purified by gel filtration chromatography on a Sephadex G-200 column. The purified product had 10 μg of FITC/mg of LPS. It displayed an emission maximum at 520 nm upon excitation at 495 nm. Polymyxin B sulfate was purchased from Sigma Chemical Co. and used without further purification.

Methods. Preparation of dansyl- and Rhodamine-Labeled PMB. 5-Dimethylaminonaphthalene-1-sulfonyl-labeled PMB (dansyl-PMB) was prepared as described earlier by Schindler and Teuber.[24] The dansyl-PMB complexed to LPS had an emmision maximum at 495 nm when excited at 340 nm. Rhodamine-labeled PMB was prepared by adding lissamine rhodamine sulfonyl chloride (Molecular Probes) to PMB (1 mM) in 10 mM $NaHCO_3$ solution. This was stirred in the dark for 4 h, and the excess label was removed by gel filtration on a Sephadex G-25 column, dialyzed against deionized water for 48 h, and lyophilized. The HPLC profile showed a single broad peak when eluted through a reversed-phase C-18 column, using methanol−water (1:8). Upon excitation at 465 nm, the emission was observed at 580 nm, characteristic of a rhodamine label.

All the LPS samples in the appropriate buffer were vortexed for 10 min at 70 °C and mixed with equimolar quantities of triethylamine with respect to anionic groups in them. Samples were sonicated at room temperature using a Braun sonicator for 5 min prior to use.

(42) Craig, L. C. *Science* **1968**, *144*, 1093−1099.
(43) Gibbons, W. A.; Alms, H.; Bockman, R. S.; Wyssbrod, H. R. *Biochemistry* **1972**, *11*, 1721−1725.
(44) Vara, M.; Vara, T. *Nature* **1983**, *309*, 526−528.
(45) Kubesh, P.; Boggs, J.; Luciano, L.; Maas, G.; Tummler, B. *Biochemistry* **1987**, *26*, 2139−2149.
(46) Lio, S.-Y.; Ong, G.-T.; Wang, K.-T.; Wu, S.-H. *Biochim. Biophys. Acta* **1995**, *1252*, 312−320.
(47) David, S. A.; Awasthi, S. K.; Wiese, A.; Ulmer, A. J.; Lindner, B.; Brandenburg, K.; Seydel, U.; Rietschel, E. Th.; Sonesson, A.; Balaram, P. *J. Endotoxin. Res.* **1996**, *3* (5), 369−379.
(48) Galanos, C.; Luderitz, O.; Westphal, O. *Eur. J. Biochem*. **1969**, *93*, 1463−1464.

Fluorescence Measurements. All fluorescence measurements were made using a Jasco FP-777 spectrofluorometer. A slit width of 5 nm for both monochromators was used. The samples and the cell were maintained at a constant temperature (±0.1 °C) using a Lauda water bath. An average of 10 measurements were taken for each reading.

For determining the association constants for the binding of dansyl-PMB to LPS, defined concentrations of dansyl-PMB in 50 mM phosphate buffer (pH 7.2) were titrated with a fixed concentration of LPS (10 μM) in the same buffer. In studies involving the fluorescence resonance energy transfer (FRET), the rhodamine-labeled PMB complexed with fluorescein-tagged LPS was excited at 495 nm, and the emission characteristics of rhodamine were monitored at 580 nm.The measurements were made after an interval of 2 min to allow for the completion of the reaction. The association constants were evaluated as described by Chipman et al.[35]

Kinetic Studies. Fast reaction kinetic experiments in the fluorescence mode were performed on an Applied Photophysics SX.18MV stopped-flow apparatus (Leatherhead, KT227PB, UK). The dead time of the instrument was measured as described by Tonomura et al.[49] and was found to be 1.2 ms. For dansyl-PMB−LPS interactions, the samples were excited at 340 nm, and emission was monitored beyond 420 nm, by using a cutoff filter, at right angles to the excitation beam. For kinetic measurements involving FRET between fluorescein−LPS and rhodamine-labeled PMB, the sample were excited at 495 nm, and emission was studied beyond 560 nm using a cutoff filter. The sample syringes and the cell were maintained at a constant temperature (±0.1 °C) by means of water bath, through jackets surrounding the cell and syringes. Unless otherwise stated, all measurements were made in 50 mM sodium phosphate buffer, pH 7.2. For measuring the effects of the ionic strength on the kinetic parameters, experiments were conducted by adding varying concentrations of NaCl. All traces are cumulative average of 5−10 successive kinetic profiles. The analysis of the stopped-flow traces were done by curve-fitting using the Marquardt algorithm based on the routine curves. All curves were fitted to mono-, bi-, and triexponential equations, with floating end points. All curve-fitting and subsequent analysis was done using an ARCON 5000, RISC workstation supplied by the manufacturer.

Acknowledgment. This work has been supported by a grant from the Department of Science and Technology, Government of India to A.S. B.P.G. is a Research associate in the above grant. The authors gratefully acknowledge the critical comments offered by Prof. S. K. Podder. The stopped-flow instrument is provided by the Department of Biotechnology, Government of India, to A.S.

JA981777J

(49) Tonomura, B.; Nakatani, H.; Ohnishi, M.; Yamaguchi-Ito, J.; Hiromi, K. *Biochemistry* **1978**, *84*, 370−383.